



Fusion of glacier displacement observations with different temporal baselines

Laurane Charrier, Y Yan, Elise Colin-Koeniguer, E. Trouvé

► To cite this version:

Laurane Charrier, Y Yan, Elise Colin-Koeniguer, E. Trouvé. Fusion of glacier displacement observations with different temporal baselines. IGARSS 2021, Jul 2021, Bruxelles, Belgium. 10.1109/IGARSS47720.2021.9553831 . hal-03340445

HAL Id: hal-03340445

<https://hal.science/hal-03340445>

Submitted on 10 Sep 2021

HAL is a multi-disciplinary open access archive for the deposit and dissemination of scientific research documents, whether they are published or not. The documents may come from teaching and research institutions in France or abroad, or from public or private research centers.

L'archive ouverte pluridisciplinaire **HAL**, est destinée au dépôt et à la diffusion de documents scientifiques de niveau recherche, publiés ou non, émanant des établissements d'enseignement et de recherche français ou étrangers, des laboratoires publics ou privés.

FUSION OF GLACIER DISPLACEMENT OBSERVATIONS WITH DIFFERENT TEMPORAL BASELINES

L. Charrier^{1,2}, Y. Yan¹, E. Colin-Koeniguer², E. Trouv  ¹

¹ Universit   Savoie Mont Blanc, LISTIC, Annecy France ² ONERA, DTIS, Paris, France

ABSTRACT

This article proposes a method based on the temporal closure of the displacement measurement's network. The aim is to extract short-term glacier velocities and to use data redundancy to reject outliers and reduce uncertainty. By using all the available displacement measurements, we retrieve a displacement time series between consecutive observation dates by means of an inversion. The proposed inversion method is an Iterative Weighted Least Square (IWLS) with a regularization on the discrete derivative of displacements. We apply our method to a glaciers velocity data-set covering Fox Glacier in the Southern Alps of New Zealand.

Index Terms— Glacier, velocity, time series, fusion

1. INTRODUCTION

Velocity maps are necessary to precisely monitor ice dynamics, to infer sub-glacial processes and/or ocean forcing, and to derive other products such as mass-balance or strain rates when the amount of data is sufficient. Nowadays, a lot of satellite image derived scene-pair ice velocities tend to be available online [1, 2] or on-demand [3]. This amount of data is complex to analyze since velocity measurements span different temporal baselines. Indeed, velocities covering small temporal baselines are close to the temporal derivative of the position whereas long temporal baseline velocities approximate the mean velocity over the considered period. Moreover, the uncertainty of velocity measurements differs. In case of small temporal baselines, the uncertainty can be large due to the small displacement magnitude, while in case of long temporal baselines, the uncertainty mainly results from the surface change between image acquisitions.

Some authors chose to overcome this problem by picking small or long temporal baselines depending on their interest (small temporal baselines for intra-annual or long temporal baselines for inter-annual studies) [4]. This implies having enough data which cannot always be possible, especially in mountain areas. Therefore, other authors suggested integrating a regression function to fit displacement measurements [5] which requires a priori knowledge of the displacement behavior.

In this paper, we propose a temporal inversion method based on the temporal closure of the displacement measurement's network. This kind of approach was originally developed for InSAR time series [6]. Later, it has been applied to SAR speckle-tracking [7] and optical cross-correlation displacement measurements [8]. However, it has mostly been applied to almost linear displacement in case of sufficient redundancy. Moreover, taking the uncertainty of different displacement measurements into account remains an open question. Here, the main objective is to deal with the cases of more complex displacement behavior (e.g. seasonal variability) and without large redundancy for the whole period under consideration. We suggest to use all the available displacement measurements to obtain a displacement time series between consecutive observation dates. For that, we propose 1) an IWLS with a regularization on the discrete derivative of the displacement and 2) an appropriate weighting function, inspired from [9], for different displacement measurements in case of unknown uncertainty. The proposed method is illustrated on the Fox Glacier situated in the Southern Alps of New Zealand. The final goal is to extract the short-term glacier velocity evolution with reduced uncertainty as in [10].

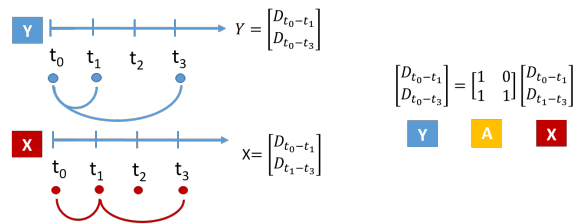


Fig. 1: Illustration of the temporal closure of the displacement measurement's network. The vector Y corresponds to the observed displacements. The vector X stands for the displacement time series between consecutive dates. A is the design matrix linking the vectors X and Y.

2. DATA AND STUDY AREA

The study area is the Southern Alps of New Zealand. We apply the proposed method to the Fox glacier, a fast-flowing, temporal maritime glacier [11, 12].

The considered data-set is from [3]. It contains velocity measurements computed with a modified version of the cross-correlation algorithm *Ampcor* from NASA. A first outlier-removal has been carried out. Pixel offsets that deviate more than three units from the offsets filtered by a 9 pixels x 9 pixels median filter have been removed. We consider Sentinel-2 data having a spatial resolution of 10 m and a repeat period of 5 days. The temporal baselines are ranging from 5 to 100 days and from 330 to 400 days. The resulting velocity maps have a 50 m spatial resolution. The measurements cover the period from October 2016 to December 2018.

3. METHODOLOGY

3.1. Temporal closure of displacement measurement's network

The proposed method is a pixel-based approach. The key principle relies on the redundancy of the observed displacement measurement's network. It uses the fact that displacements are additives to infer a displacement time series between consecutive dates. This is known as the Leap Frog formulation. For example, in the Figure 1, the displacement between the dates t_0 and t_1 and the dates t_0 and t_3 are overlapping. The relation between the Leap Frog time series X (of dimension p) and the observed displacements Y (of dimension n) is given by the design matrix A (of dimension $n \times p$). By solving the equation $AX = Y$, the minimized square distance between the displacements $D_{t_0-t_1}$ inferred from both $D_{t_0-t_1}$ and $D_{t_0-t_3}$ is computed.

Two configuration for the Leap Frog time series X can be considered: 1) displacements between consecutive dates included in Y (*cf.* Figure 1), 2) displacements between consecutive dates with a regular time span (e.g. the satellite repeat cycle). If the number of data in Y is not sufficient, the system is more likely to be ill-posed in this second configuration. Here, we present results from the first configuration.

3.2. Inversion

To solve the equation $AX = Y$, we propose an Iterative Weighted Least Square (IWLS) approach. A regularization term on the discrete derivative of the leap frog velocities can be added as done in [8] assuming that ice velocities have a low temporal variability on a short time scale (i.e. with a small temporal sampling). That is to say, we minimize the cost function:

$$\arg \min (\|W(AX - Y)\|^2 + \|\Gamma X\|^2) \quad (1)$$

$$\hat{X} = (A^T W A + \Gamma^T \Gamma)^{-1} A^T W Y \quad (2)$$

where Γ is a $p \times p$ matrix representing the discrete derivative operator and W a $n \times n$ matrix standing for the weight given to each value in Y . The diagonal element of Γ are $\Gamma_{k,k} = 1/\Delta\tau$

and the element above the diagonal are $\Gamma_{k,k+1} = -1/\Delta\tau$ with $\Delta\tau$ the temporal sampling.

The solution of the equation is equation 2 using a Singular Value Decomposition (SVD) when the system is ill-posed (i.e. $n < p$) [6].

This approach includes at least two iterations.

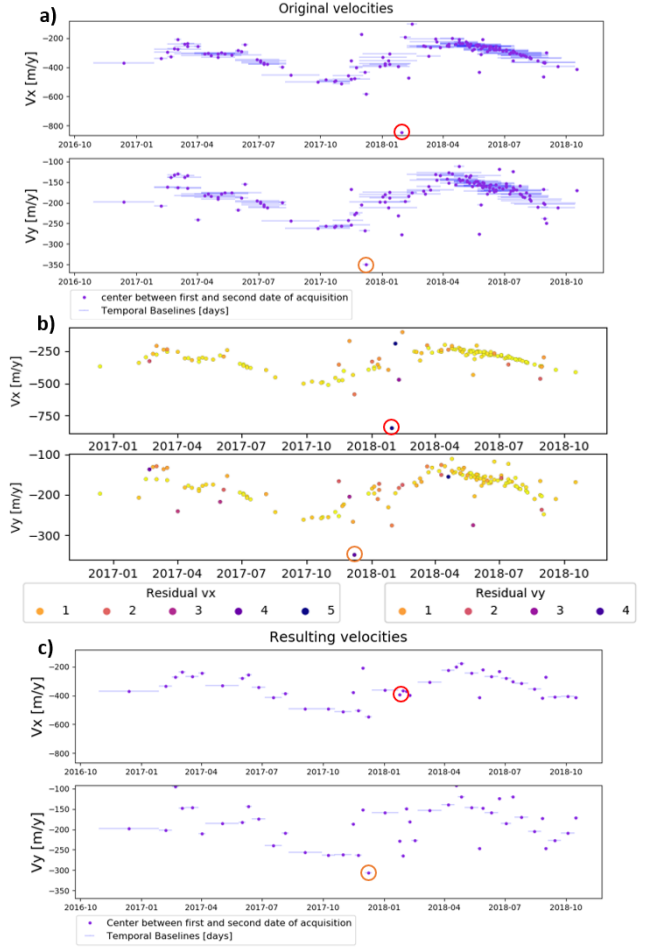


Fig. 2: Example of results for a point of coordinate (-43.532, 170.134) situated on Fox glacier. Two outliers that seem to stand out of the trend are encircled in red and orange in each plot. a) Original data for E-W (V_x) and N-S (V_y) velocity components. The purple dots represent the center between the first and second date of acquisition, the bars show the temporal baseline of each velocity. b) Internally studentized-residuals resulting from the first OLS inversion superimposed on the original data. The color represents its magnitudes in m/y. c) Results from the IWLS inversion.

3.2.1. First iteration

Indeed, the observed displacements are heteroscedastic, i.e. the variance across elements is different. Therefore, it is relevant to add a weight to each element in Y based on the variance. The weight vector is W . Because the variance is un-

known, we perform a first Ordinary Least Square (OLS) inversion (i.e. $W = I$ in equation 1 and 2) to retrieve the internally studentized-residuals vector, an indicator used to detect outliers [9], defined as:

$$Z = \frac{R}{\sigma\sqrt{1 - H}} \quad (3)$$

where R are the residuals (the difference between the reconstructed input displacements computed with $AX = Y$ and the original displacements Y) of dimension n , H the leverage vector of dimension n , i.e. the diagonal elements of the hat matrix $A(A^TWA + \Gamma^T\Gamma)^{-1}A^TW$, \cdot the element wise division and $\sigma = \sum_{i=1}^n \frac{R_i^2}{(n-p)}$ the standard deviation of residuals.

3.2.2. Next iteration

Then, a second inversion is performed where W is defined using the Tukey's biweight function, which is a common down-weight function [9]. The diagonal elements of W are defined as:

$$W^{k,k} = \begin{cases} [1 - (z^{k,k}/c)^2]^2, & |z^{k,k}| < c \\ 0, & |z^{k,k}| > c \end{cases} \quad (4)$$

where c is a tuning constant which is usually set to 4.685, producing 95% efficiency at a normal distribution [13].

Then, other Weighted Least Square iterations are performed where W is updated with the result from the previous iteration. The algorithm stops when $\text{mean}(|\hat{X}^i - \hat{X}^{i-1}|) < \delta$ where \hat{X}^i corresponds to the results of a given iteration and \hat{X}^{i-1} the results of the previous one. δ is a predefined threshold, here set to 0.05 m.

On the one hand, by weighting the Least Square inversion, our results tend to be robust to outliers which will have larger internally studentized-residuals. On the other hand, the regularization term allows reducing the outliers by decreasing abrupt variability where the IWLS inversion is weakly constrained.

4. RESULTS

4.1. Temporal analysis

The temporal analysis is illustrated on a point situated on Fox Glacier at location (-43.532, 170.134). The W-E and N-S components (V_x and V_y respectively) of the velocity are plotted in Figure 2a).

The internally studentized-residuals obtained from the first OLS inversion are shown in Figure 2b). Their values are higher when the original data appear as outliers such as the point with a V_x below -750 m/y in 2018-02 (red circle) and the point with a V_y lower than -300 m/y in 2017-12 (orange circle). By using the internally studentized-residuals as weights in a second inversion, the final results are less impacted by outliers (cf. Figure 2c).

Furthermore, the internally studentized-residuals could be used as a proxy of the uncertainty in velocity measurements. This can be especially of interest concerning glaciers. Indeed, authors usually access the uncertainty of a velocity map by computing the standard deviation of displacements on a stable or slow-moving ground where the displacement value is known. However, uncertainty can be higher on glaciers due to a fast-changing surface which can cause decorrelation and match blunders [1, 3]. This can lead to underestimating the uncertainty on moving areas. The proposed internally studentized-residual overcomes this problem and proposes a more appropriate indicator of the uncertainty on moving areas.

4.2. Spatial analysis

The spatial analysis is illustrated on a rectangle of $10 \times 10 \text{ km}^2$ surrounding Fox Glacier (top left hand corner (-43.565, 170.144), bottom right hand corner(-43.565, 170,144)).

The temporal mean velocity of each pixel in the original data-set is compared with the IWLS inversion results. The latter have an averaged temporal baseline of 22 days, therefore, temporal baselines lower than 25 days are selected in the original data-set for comparison. On glaciers, our results are consistent with the original data-set and previous studies [11, 12] (cf. Figure 3). Furthermore, we find that the mean velocities on the stable ground are closer to 0 after inversion. We compute the RMSE of the velocity magnitude on stable ground as follows $RMSE = \sqrt{\frac{1}{N} \sum (V_x^2 + V_y^2)}$. V_x and V_y are the velocities recorded for each pixel and each temporal baseline, N is the length of V_y and V_x (i.e. the number of pixels times p). We find an RMSE of 149.3 m/y before inversion and 82.1 m/y after.

5. CONCLUSION

In this paper, we propose a method based on the temporal closure of the displacement measurement's network. The goal is to infer a displacement time series between consecutive observation dates from all the available displacements in order to extract short-term glacier velocity evolution with a reduced uncertainty. This method takes advantage of the data redundancy and relies on an IWLS algorithm and a regularization on the discrete derivative of displacements. Moreover, we proposed the internally studentized-residuals for weighting the displacement measurements of different quality, which is of particular interest in case of unknown data uncertainty. We have shown that our method was robust to outliers. Moreover, both temporal and spatial analyses reveal that the inversion reduces the noise.

A follow-on of this study will be to fuse displacements from different sensors and to explore the possibility to add a spatial constraint inside the inversion. In future works, we will also apply our method to other data-sets and regions.

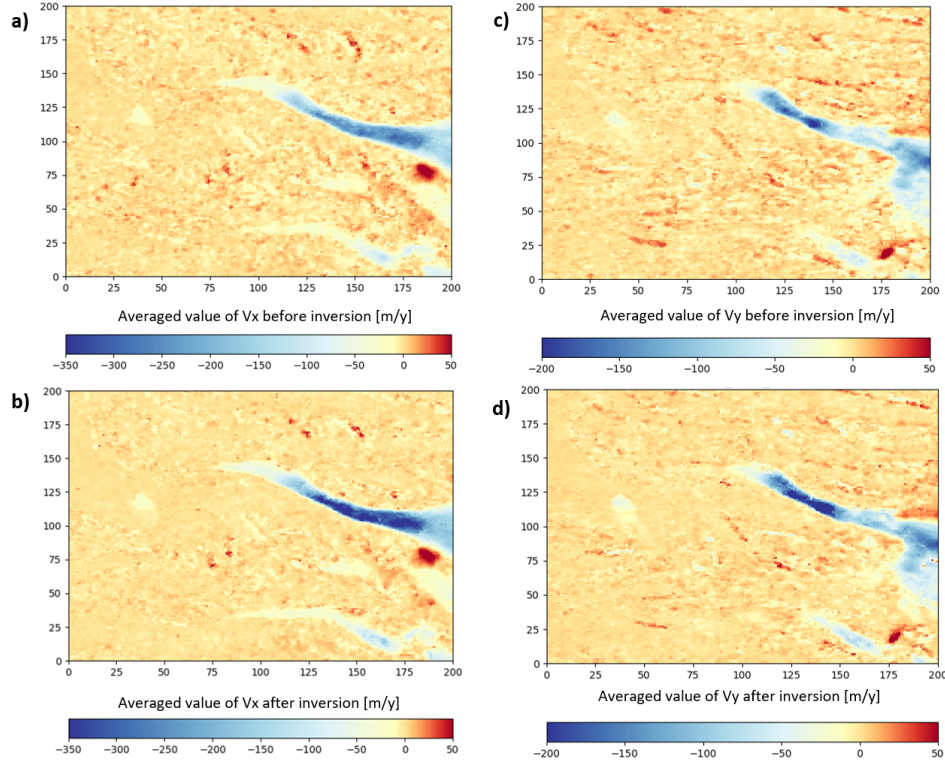


Fig. 3: Mean velocities for each pixel for a) the W-E component (V_x) of the original velocities b) V_x of the inverted velocities c) the N-S component (V_y) of the original velocities d) V_y of the inverted velocities. The considered area is a rectangle of 10×10 km surrounding Fox Glacier (top left hand corner (-43.565, 170.144), bottom right hand corner(-43.565, 170,144)).

Acknowledgments. Ice velocity were processed by Millan R. and Mouginot J. thanks to a post-doctoral fellowship from the CNES and the CNES MaiSON project.

6. REFERENCES

- [1] Alex S Gardner, Geir Moholdt, Ted Scambos, Mark Fahnestock, Stefan Lüttenberg, Michiel Van Den Broeke, and Johan Nilsson, “Increased west antarctic and unchanged east antarctic ice discharge over the last 7 years,” *Cryosphere*, vol. 12, no. 2, pp. 521–547, 2018.
- [2] Mark Fahnestock, Ted Scambos, Twila Moon, Alex Gardner, Terry Haran, and Marin Klinger, “Rapid large-area mapping of ice flow using landsat 8,” *Remote Sensing of Environment*, vol. 185, pp. 84–94, 2016.
- [3] Romain Millan, Jérémie Mouginot, Antoine Rabatel, Seongsu Jeong, Diego Cusicanqui, Anna Derkacheva, and Mondher Chekki, “Mapping surface flow velocity of glaciers at regional scale using a multiple sensors approach,” *Remote Sensing*, vol. 11, no. 21, pp. 2498, 2019.
- [4] Anna Derkacheva, Jeremie Mouginot, Romain Millan, Nathan Maier, and Fabien Gillet-Chaulet, “Data reduction using statistical and regression approaches for ice velocity derived by landsat-8, sentinel-1 and sentinel-2,” *Remote Sensing*, vol. 12, no. 12, pp. 1935, 2020.
- [5] Chad A Greene, Alex S Gardner, and Lauren C Andrews, “Detecting seasonal ice dynamics in satellite images,” *The Cryosphere*, vol. 14, no. 12, pp. 4365–4378, 2020.
- [6] Paolo Berardino, Gianfranco Fornaro, Riccardo Lanari, and Eugenio Sansosti, “A new algorithm for surface deformation monitoring based on small baseline differential sar interferograms,” *IEEE Transactions on geoscience and remote sensing*, vol. 40, no. 11, pp. 2375–2383, 2002.
- [7] Francesco Casu, Andrea Manconi, Antonio Pepe, and Riccardo Lanari, “Deformation time-series generation in areas characterized by large displacement dynamics: The sar amplitude pixel-offset sbas technique,” *IEEE Transactions on Geoscience and Remote Sensing*, vol. 49, no. 7, pp. 2752–2763, 2011.
- [8] Noelia Bontemps, Pascal Lacroix, and Marie-Pierre Doin, “Inversion of deformation fields time-series from optical images, and application to the long term kinematics of slow-moving landslides in peru,” *Remote Sensing of Environment*, vol. 210, pp. 144–158, 2018.
- [9] Hongyu Liang, Lei Zhang, Xiaoli Ding, Zhong Lu, Xin Li, Jun Hu, and Songbo Wu, “Suppression of coherence matrix bias for phase linking and ambiguity detection in mtinsar,” *IEEE Transactions on Geoscience and Remote Sensing*, 2020.
- [10] Bas Altena, Ted A Scambos, Mark Fahnestock, and Andreas Kääb, “Extracting recent short-term glacier velocity evolution over southern alaska and the yukon from a large collection of landsat data,” *The Cryosphere*, vol. 13, no. 3, pp. 795–814, 2019.
- [11] HL Purdie, MS Brook, and IC Fuller, “Seasonal variation in ablation and surface velocity on a temperate maritime glacier: Fox glacier, new zealand,” *Arctic, Antarctic, and Alpine Research*, vol. 40, no. 1, pp. 140–147, 2008.
- [12] Andreas Kääb, Solveig H Winsvold, Bas Altena, Christopher Nuth, Thomas Nagler, and Jan Wuite, “Glacier remote sensing using sentinel-2. part i: Radiometric and geometric performance, and application to ice velocity,” *Remote Sensing*, vol. 8, no. 7, pp. 598, 2016.
- [13] Peter J Huber, “Robust estimation of a location parameter,” in *Breakthroughs in statistics*, pp. 492–518. Springer, 1992.